6 FT
6
5
5
4
3
2
1

DETERMINATION OF LOAD DISTRIBUTION ON A BEAM FROM MEASUREMENTS ON ITS DEFLECTED FORM

PAUL ANDERSEN, Ph.D.
Professor of Structural Engineering
SANTOSH K. MUKHOPADHYAY, Ph.D.

BULLETIN NO. 31

UNIVERSITY OF MINNESOTA
J. L. MORRILL, President
INSTITUTE OF TECHNOLOGY
A. F. SPILHAUS, Dean
ENGINEERING EXPERIMENT STATION
F. B. ROWLEY, Director

VOL. LIII NO. 1 JANUARY 4, 1950

Entered at the post office in Minneapolis as semi-monthly second-class matter, Minneapolis, Minnesota. Accepted for mailing at special rate of postage provided for in Section 1103, Act of October 3, 1917, authorized July 12, 1918.

ACKNOWLEDGMENT

This bulletin is the result of research sponsored by the Engineering Experiment Station of the University of Minnesota.

The apparatus, which furnished the experimental data upon which this study is based, was designed and built under the direction of the senior author prior to the entry of the United States into World War II. Due to war activities it was not made available for tests until 1947. The actual work of loading and recording observations was performed by the junior author as part of his theses for the degrees of Master of Science and Doctor of Philosophy.

The authors gratefully acknowledge the help and encouragement given by Professor Frank B. Rowley and Professor C. E. Lund of the Engineering Experiment Station of the University of Minnesota.

TABLE OF CONTENTS

	Page
Introduction	ix
Review of Theory	1
Use of Power Series	1
Method of Least Squares	6
Determination of Load Diagram	7
Deflection Function	7
Curvature Function	9
Test Apparatus	11
Earth Pressure Box	11
Measurements of Deflections	11
Recording of Bending Strains	12
Curvature Readings	15
Test Procedure	16
Test Observations	18
Sequence of Loading	18
Records of Observations	19
Auxiliary Tests	22
Computations	24
Use of Deflections	24
Curvature and Moment	25
Comparison of Results	38
Deflections and Strains	38
Passive Pressures	40
Curvature	40

ILLUSTRATIONS

Figure		Page
1.	Variable Load Intensity on Portion of Beam	3
2.	Curve Fitting	3
3.	Beam Dimensions	8
4.	Details of Earth Pressure Box	10
5.	End View of Earth Pressure Box	12
6.	Location of Strain Gages on Two Surfaces of Aluminum Plate	13
7.	Diagrams Explaining Switch	14
8.	Instrument for Curvature Measurement	15
9.	Notation for Curvature Measurement	16
10.	Top View of Loaded Membrane	17
11.	The Different Cases of Loading Observed	18
12.	Test Results for Determining the Modulus of Elasticity	23
13.	Pressure Diagrams Obtained from Measured Deflections	39
14.	Pressure Diagrams Obtained from Measured Strains	39
15.	Pressure Diagrams Obtained from Measured Strains	42
16.	Pressure Diagrams Obtained from Measured Curvatures	42

TABLES

Number		Page
I	General Expressions for k's and K's in Terms a, l and A's	4
II	Mean Net Deflection in Inches	20
III	Curvature Readings: Rise, b, (see Figure 9) in 1/1000 inch	21
IV	Net Strain Gage Readings in Micro-Inches Per Inch	22
V	Evaluation of Coefficients in Equation (19)	25
VI	Evaluation of C_1 from Deflections in Table II	27
VII	Evaluation of C_2 from Deflections in Table II	28
VIII	Evaluation of Coefficients in Equation (27)	31
IX	Evaluation of C_1' from Curvature Readings in Table III	33
X	Evaluation of C_2' from Curvature Readings in Table III	34
XI	Evaluation of C_1' from Strain Gage Readings in Table IV	36
XII	Evaluation of C_2' from Strain Gage Readings in Table IV	37
XIII	Comparison of Fitness	41
	A. By Measured Deflections	
	B. By Measured Strains	
	C. By Measured Curvatures	

INTRODUCTION

Structural design can usually be divided into two parts: the evaluation of the forces that must be resisted by the structure and the determination of stresses which these forces produce.

For most structures the given forces are known or easily calculated. In the cases of gravity loads and hydrostatic pressures the results of the evaluations are precise and unmistakable. In the cases of other types of loads, however, considerable uncertainty exists regarding the proper magnitudes of the loads to be resisted. Examples of the latter are such forces as: lateral earth pressures, grain pressures on the walls of silos and bins, wind pressures, earthquake forces and impact loads.

It is the object of this paper to present a method of finding such unknown forces by measuring the deflections and strains produced on a structure by these forces and reversing the usual order of structural computations.

REVIEW OF THEORY

As the object of this bulletin is an attempt to establish the intensities of load by a mathematical interpretation of their effects (in terms of stress and strain) on a highly flexible beam, it is desirable to review briefly the methods for finding the relationships existing between quantities whose corresponding values have been obtained by experiments.

Use of power series—Figure 1 shows a beam, AC, fixed at one end and simply supported (free to rotate) at the other end. This beam is assumed to be subjected to the action of a continuous load of varying intensity over a portion, BC, of its span. In such a beam it is known that the load intensities can be found by successive differentiation of the deflections thus:

$$p = EI \frac{d^4y}{dx^4} \qquad (1a)$$

If the product EI is constant, the following relations involving respectively shearing force, V, bending moment, M, slope and deflection are obtained by consecutive integrations:

$$V = EI \frac{d^3y}{dx^3} = \int p\,dx$$

$$M = EI \frac{d^2y}{dx^2} = \int\int p\,dx\,dx$$

$$EI \text{ (slope)} = EI \frac{dy}{dx} = \int\int\int p\,dx\,dx\,dx$$

$$EI \text{ (deflection)} = EI\,y = \int\int\int\int p\,dx\,dx\,dx\,dx \qquad (1b)$$

Suitable limits and integration constants must, of course, be introduced.

In the case of the beam shown in Figure 1, the load intensity is zero on the left portion, AB, and varies on the right portion, BC. If it is assumed that this variation can be expressed by a polynomial, then Equation 1 can be written for the two parts thus:

AB: $$EI \frac{d^4y}{dx^4} = 0 \qquad (2a)$$

BC: $$EI \frac{d^4y}{dx^4} = \sum A_n x^n ; n = 0, 1, 2, \ldots . \qquad (2b)$$

Integrating gives

$$EIy = k_1 \frac{x^3}{6} + k_2 \frac{x^2}{2} + k_3 x + k_4 \qquad (3a)$$

$$EIy = \sum \frac{A_n x^{n+4}}{(n+1)(n+2)(n+3)(n+4)} + K_1 \frac{x^3}{6} + K_2 \frac{x^2}{2} + K_3 x + K_4 \qquad (3b)$$

The eight constants of integration in the above equations may be determined from the following conditions:

At A ($x = 0$): $y = 0$, $EI \frac{d^2y}{dx^2} = M_A$

At B ($x = a$): Identical values are obtained from Equations (3a) and (3b) for y, $\frac{dy}{dx}$, $\frac{d^2y}{dx^2}$, $\frac{d^3y}{dx^3}$

At C ($x = 1$): $y = 0$, $\frac{dy}{dx} = 0$

If these conditions are imposed, the values for the coefficients k and K are readily determined from the resulting eight simultaneous equations. The general expressions for these values

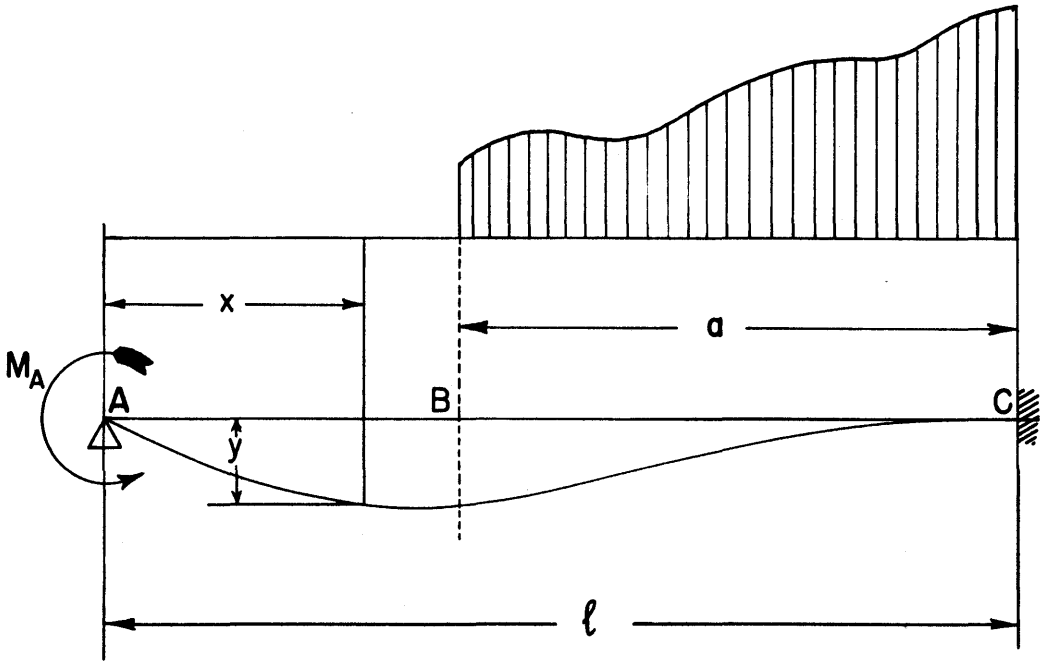

FIG. 1: VARIABLE LOAD INTENSITY ON PORTION OF BEAM.

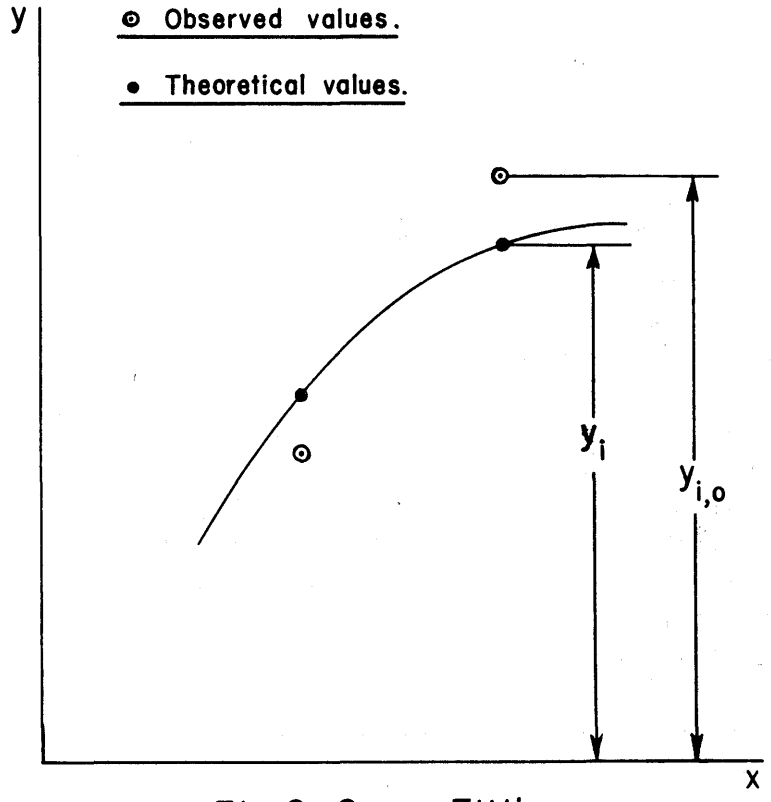

Fig. 2: Curve Fitting.

TABLE I

GENERAL EXPRESSIONS FOR k's AND K's IN TERMS OF a, ℓ, AND A's

$$k_1 = \sum A_n \left[-\frac{3\ell^{n+1}}{(n+1)(n+2)(n+4)} - \frac{a^{n+1}}{n+1} - \frac{3a^{n+2}}{2\ell(n+2)} - \frac{a^{n+4}}{2\ell^3(n+4)} \right] - \frac{3M_A}{2\ell}$$

$$k_2 = M_A$$

$$k_3 = \sum A_n \left[\frac{\ell^{n+3}}{2(n+2)(n+3)(n+4)} + \frac{a^{n+3}}{2(n+3)} - \frac{\ell a^{n+2}}{4(n+2)} - \frac{a^{n+4}}{4\ell(n+4)} \right] - \frac{\ell M_A}{4}$$

$$k_4 = 0$$

$$K_1 = \sum A_n \left[-\frac{3\ell^{n+1}}{(n+1)(n+2)(n+4)} - \frac{3a^{n+2}}{2\ell(n+2)} - \frac{a^{n+4}}{2\ell^3(n+4)} \right] - \frac{3M_A}{2\ell}$$

$$K_2 = \sum \left[A_n \frac{\ell^{n+2}}{(n+2)} \right] + M_A$$

$$K_3 = \sum A_n \left[\frac{\ell^{n+3}}{2(n+2)(n+3)(n+4)} - \frac{\ell a^{n+2}}{4(n+2)} - \frac{a^{n+4}}{4\ell(n+4)} \right] - \frac{\ell M_A}{4}$$

$$K_4 = \sum A_n \left[\frac{\ell^{n+4}}{6(n+4)} \right].$$

have been listed in Table I and the deflection function for the beam can be written thus for the case in Figure 1 for the unloaded portion AB:

$$EIy = A_1 f_1(x) + A_2 f_2(x) + A_3 f_3(x) + \ldots \quad \ldots \quad \ldots \qquad (4a)$$

and for the loaded portion BC:

$$EIy = A_1 F_1(x) + A_2 F_2(x) + A_3 F_3(x) + \ldots \quad \ldots \quad \ldots \qquad (4b)$$

In these two equations the unknown coefficients, A, can be found if a sufficient number of deflections are determined by observation. Usually there are more known deflections than unknown coefficients; in which case the problem becomes one of finding the set of coefficients which will most closely represent the observed deflected beam.

If, as was done in the tests reported in this bulletin, the curvature of the beam or a set of bending moments were found by direct measurements, the variation of the second derivative would be known and only two differentiations would be required for the determination of the variation of load intensity. The number of integration constants would be reduced to four, thus

$$EI\frac{d^2y}{dx^2} = k_1 x + k_2 \qquad (5a)$$

$$EI\frac{d^2y}{dx^2} = \sum \frac{A_n x^{n+1}}{(n+1)(n+2)} + K_1 x + K_2 \qquad (5b)$$

for the unloaded and the loaded portions of the beam respectively. The values of the coefficients k_1, k_2, K_1, K_2 are listed in Table I, and if substituted in Equation 5, the variation of the second derivative can be expressed as follows for the portions AB and BC respectively:

$$EI\frac{d^2y}{dx^2} = A_1 g_1(x) + A_2 g_2(x) + A_3 g_3(x) + \ldots \quad \ldots \qquad (6a)$$

$$EI\frac{d^2y}{dx^2} = A_1 G_1(x) + A_2 G_2(x) + A_3 G_3(x) + \ldots \quad \ldots \qquad (6b)$$

Method of least squares--There are several methods available for fitting curves to observational data. The most useful and the one most frequently applied is the method of least squares. This method has the advantage of giving a unique set of values to the coefficients A in Equations (4) and (6). Furthermore, the coefficients found by least squares give the most probable relationship in the sense that the values of y computed from it are the most probable quantities of the observations, if it is assumed that the residuals $y_i - y_{i,o}$ (see Figure 2) follow the Gaussian law of errors.

Referring to Figure 2, the principle of least squares asserts that the curve which will best represent the observational data is that for which the sum of the squares of the residuals

$$\sum (y_i - y_{i,o})^2 \; ; \; i = 1, 2, 3, \ldots .$$

is a minimum. It follows that the unknown coefficients can be found by differentiating this quantity with respect to each one of them and equating to zero, thus

$$\sum (y_i - y_{i,o}) \frac{\partial (y_i - y_{i,o})}{\partial A_1} = 0$$

$$\sum (y_i - y_{i,o}) \frac{\partial (y_i - y_{i,o})}{\partial A_2} = 0 \qquad (7)$$

$$\ldots \quad \ldots \quad \ldots \quad \ldots \quad \ldots$$

Completing the differentiations gives

$$\sum (y_i - y_{i,o}) f_1(x) = 0$$

$$\sum (y_i - y_{i,o}) f_2(x) = 0 \qquad (8)$$

$$\ldots \quad \ldots \quad \ldots \quad \ldots$$

These equations are subsequently solved for A_1, A_2, A_3, ...

DETERMINATION OF LOAD DIAGRAM

From the general expressions for beam deflections and curvature, more specific relationship can be derived when distances, dimensions and elastic properties are known. Figure 3 illustrates the length, size and loaded portion of the aluminum plate which was used in the tests reported in this bulletin. As the modulus of elasticity of the aluminum was found to equal 9,774,500 pounds per square inch, the product of modulus of elasticity and the moment of inertia will equal

$$EI = 9.7745 \times 10^6 \times 12^2 \times \frac{\frac{1}{12} \times \left(\frac{1}{8}\right)^3}{12^4} = 11.0479 \text{ lb-ft}^2 \text{ per in. width}$$

In the following, this numerical value has been substituted for EI in Equations (4) and (6).

Deflection function--If it is assumed that the variation of load intensity on the aluminum plate in Figure 3 can be satisfactorily represented by a third degree polynomial, then Equation (2b) can be written

$$p = A_0 + A_1 x + A_2 x^2 + A_3 x^3 \tag{9}$$

The condition

$$A_0 = -3A_1 - 9A_2 - 27A_3 \tag{10}$$

which follows from the assumption that $p = 0$ for $x = 3$, eliminates the coefficient A_0 from the deflection function, Equations (4a) and (4b). In the following, numerical values of $l = 5.5$ feet, $a = 3$ feet, and $n = 3$ feet have been substituted in the general expressions in Table I. Thus, for AB in Figure 3,

$$y = A_1(.05357x - .00222x^3) + A_2(.37833x - .01553x^3) + A_3(2.03275x + .08287x^3) + M_A(-.12445x + .04526x - .00411x^3) \tag{11}$$

and for the portion BC,

$$y = A_1(-.18328 + .35904x - .20365x^2 + .06567x^3 - .01132x^4 + .00075x^5) + A_2(-.91641 + 1.84459x - .91642x^2 + .256x^3 - .03395x^4 + .00025x^6) + A_3(-3.53473 + 7.53123x - 3.2991x^2 + .83354x^3 - .10184x^4 + .00011x^7) + M_A(-.12445x + .04526x^2 - .00411x^3) \quad (12)$$

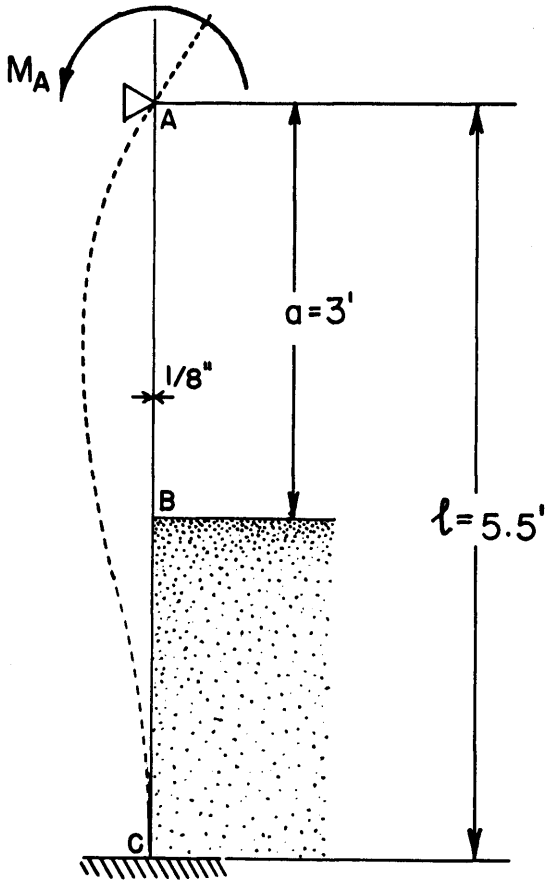

Fig. 3.

Beam Dimensions

Curvature function--In the case of curvature measurements or recording of bending strains, it was shown that only two integrations were necessary for the determination of load intensities from observed quantities. By substitution of the numerical values shown in Figure 3, the two expressions, Equations (6a) and (6b), become for AB and BC respectively

$$\frac{d^2y}{dx^2} = -.01329\ A_1x - .0132\ A_2x - .49723\ A_3x + M_A(.09052 - .02468x) \qquad (13)$$

and

$$\frac{d^2y}{dx^2} = A_1(-.4073 + .39401x - .13579x^2 + .01508x^3) + A_2(-1.83284 + 1.53598x - .40738x^2 + .00756x^3) + A_3(-6.59821 + 5.00125x - 1.22213x^2 + .00454x^3) + M_A(.09052 - .02468x) \qquad (14)$$

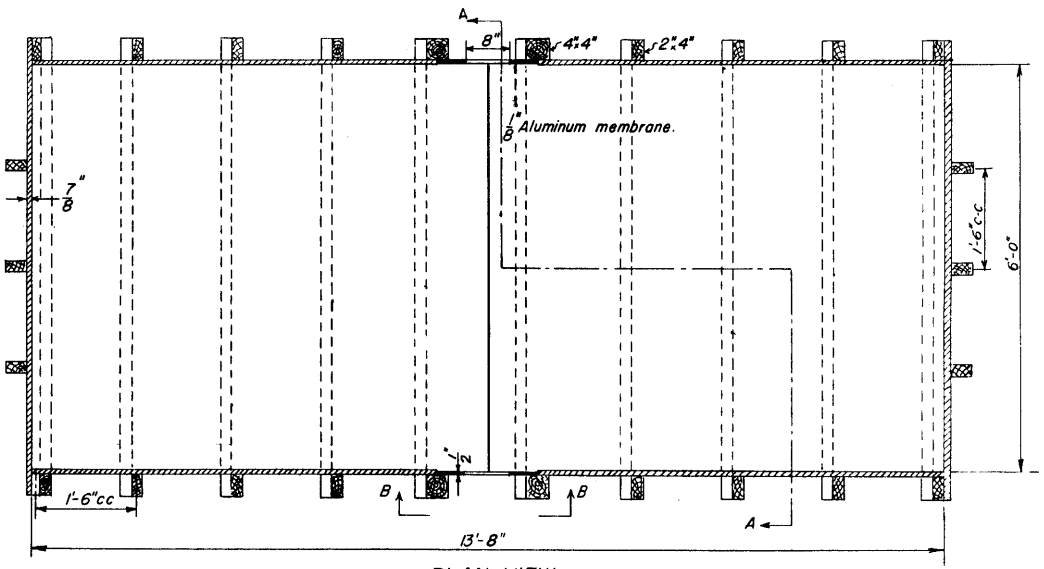

PLAN VIEW.

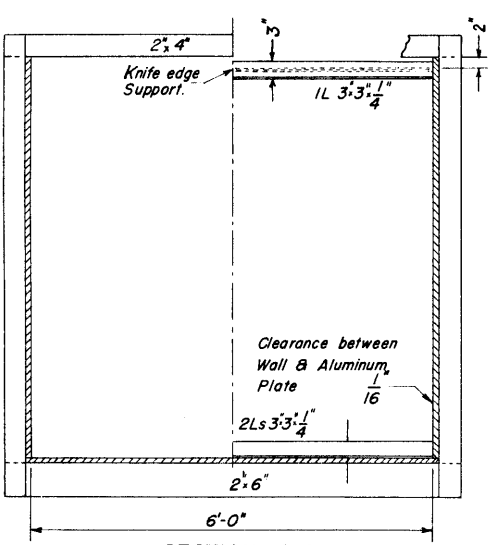

SECTION A-A.

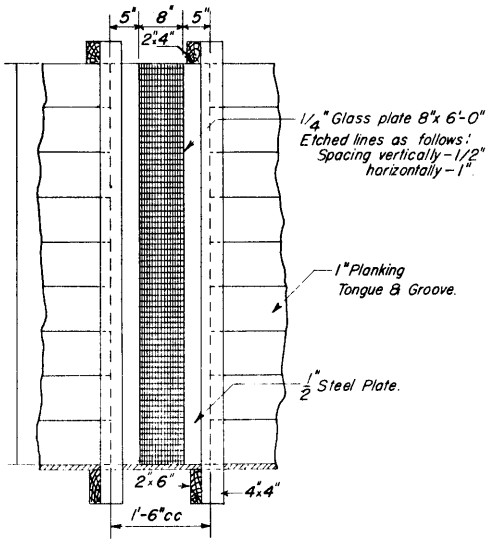

VIEW B-B.

FIG. 4.

Details of Earth-Pressure Box.

TEST APPARATUS

Earth pressure box--The lateral earth pressures were produced by dry sand inside a box of dimensions 14 feet long, 6 feet wide and 6 feet deep. As the box was located in a room of constant temperature, there were no changes of the latter during the tests.

The general arrangement of the earth pressure box is shown in Figure 4. Constructed of wood, it was divided into two equal compartments by a flexible aluminum plate of 1/8-inch thickness in the middle. The plate was fixed at the top and simply supported on a horizontal steel angle at the top of the box; it extended beyond this top support a distance of one foot. At the end of this overhang and in the center, a steel wire rope was attached, which was then carried over a pulley attached to one end of a spring dial balance. The other end of the spring balance was attached to a threaded rod which could move in either direction through a hole by tightening or loosening a nut in the form of a hand wheel. Thus, any degree of tension could be imparted to the wire rope by rotating the hand wheel, and the tension could be read on the dial of the spring balance. This tension was transmitted, through the pulley, to the end of the one-foot overhang of the plate, thereby providing a bending moment at the top support of the flexible aluminum partition plate. Thus, by varying the tension in the wire rope, any desired amount of bending moment could be imparted to the top end of the aluminum plate. In the two side walls of the box ajacent to the two edges of the flexible partition wall, two glass windows, each six inches wide and extending the full height of the box, were provided to facilitate observation of deflection and its measurement. Each glass window was etched with vertical lines one-half inch apart and horizontal lines one inch apart for convenience of measurement of deflections. At each edge, the deflections were always measured from the central vertical line on the glass window, and the difference between the initial no-load reading and the reading under load was the actual deflection due to that load.

Figure 5 shows an end view of the box which was provided with ladders for gaining access into the box. A considerable amount of bracing was incorporated in the box to enable it to withstand the lateral pressure from the sand on its sides.

Measurements of deflections--The horizontal displacements of the aluminum membrane were recorded by direct measurements through the two glass panes on the sides of the box. A steel scale graduated to one-hundredth of an inch was used. Since the measurements had to be made through the glass plate, care had to be exercised to see that there was no error due to parallax while taking

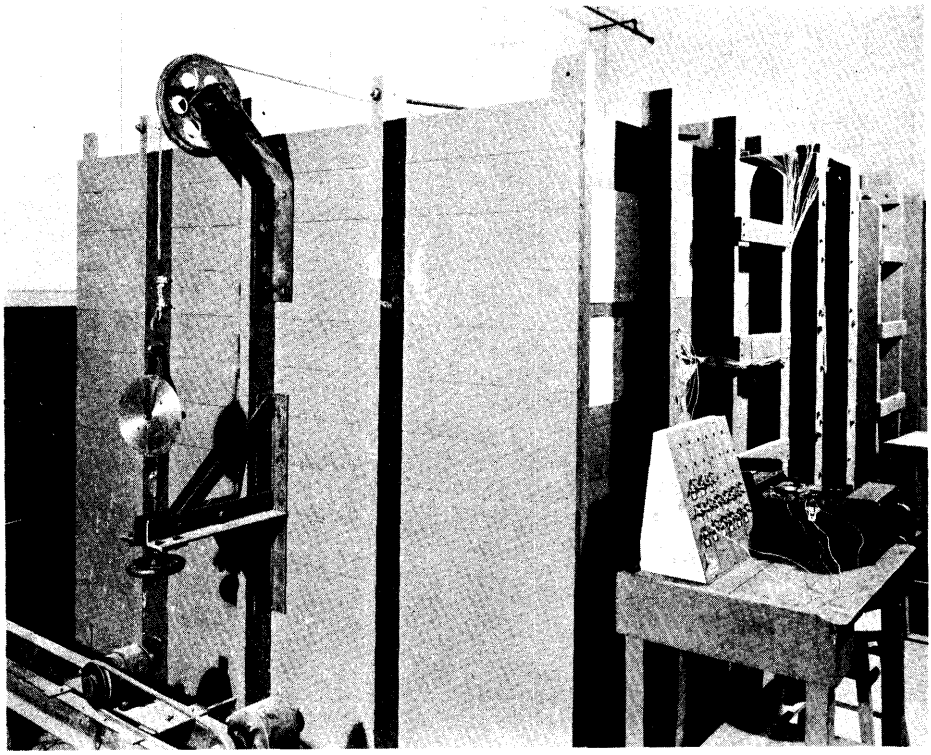

Figure 5. End view of earth pressure box.

a reading. Deflections were measured in this way at one-inch intervals along the whole length of the plate and along both edges of the plate.

Recording of bending strains--For measurement of bending strains, electrical resistance strain gages (SR-4 gages) were attached to both surfaces of the plate, according to the scheme shown in Figure 6. By this arrangement, corresponding to each gage on one face of the plate, there was another gage located exactly opposite to the former on the other face of the plate. Thus, when two such matching gages were connected, one to the terminals marked "measuring gage" and the other to the terminals marked "compensating gage," then the reading obtained in the strain indicator showed twice the value of the maximum strain due to bending moment. In this arrangement, one gage compensates the other for temperature effects, for effects due to direct tension and for effects due to direct compression, since both the gages are equally affected by all these effects. Hence, the above arrangement of gages, with one gage exactly opposite to another, measures purely bending strains, eliminating all other effects. It also magnifies the readings by

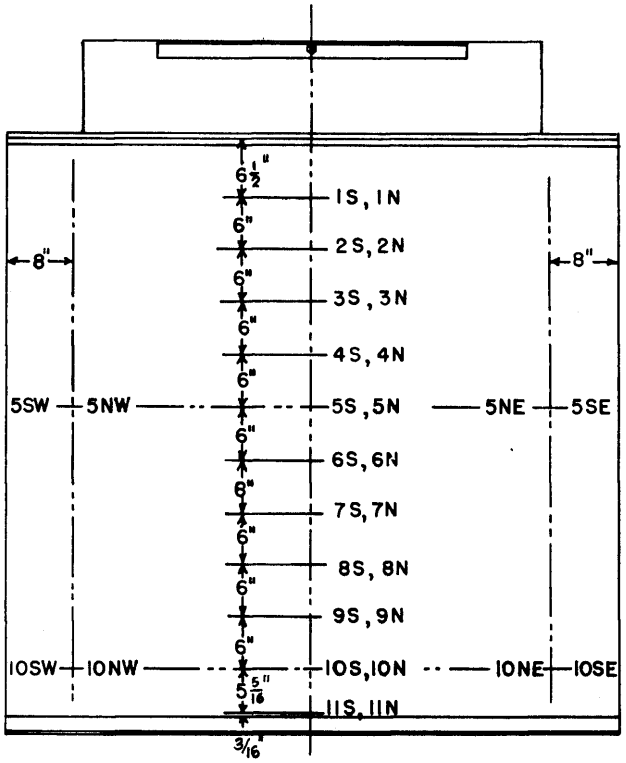

FIG. 6.
LOCATION OF STRAIN GAGES ON TWO SURFACES OF ALUMINUM PLATE.

a factor of two. Figure 7 explains the necessary switchboard connections, by means of which each pair of corresponding gages could be connected to the strain indicator by a single operation of plugging into a proper socket, one socket being marked on the switchboard for each pair of gages. Three-way jacks were used for this purpose. Since the contacts, however, were not as perfect as one would require in measurements with strain gages, the arrangement was modified by providing three binding posts, connected to the three terminals of each jack, and three wires were used to connect each trio of binding posts in turn to three terminals of the strain indicator. This meant binding of three wires every time a reading was taken, instead of just plugging in a plug; but this additional labor was justified by the accuracy attained thereby in the readings. The strain indicator used could measure a strain as small as one-millionth of an inch per inch.

In order to derive a relationship between curvature and bending strains, it should be recalled that the radius of curvature, R, is equal to the distance of the outermost fiber from the neutral axis, y, divided by the maximum fiber strain, e, thus

$$\frac{d^2y}{dx^2} = \frac{1}{R} = \frac{e}{y}$$

If R is measured in feet, e in micro-inches per inch and y in inches, it is seen that

$$\frac{1}{R} = 12 \times 10^{-6} \frac{e}{y}$$

The thickness, 2y, of the aluminum plate is one-eighth of an inch, and the recorded strain is twice the actual strain, hence

$$\frac{1}{R} = 0.000096\, e \qquad (15)$$

where e is the strain indicator reading.

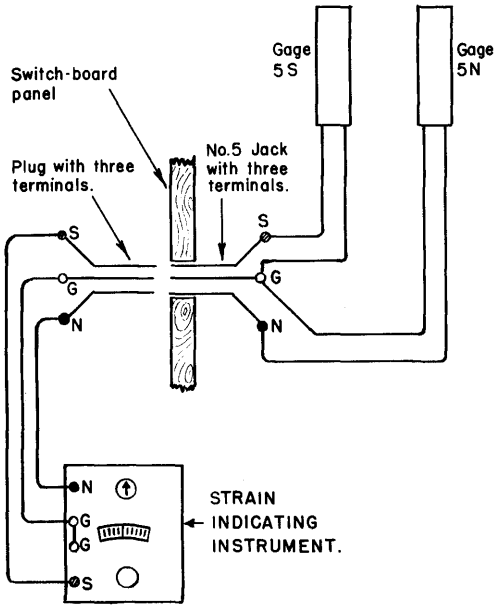

(a)
CONNECTIONS TO A TYPICAL JACK.

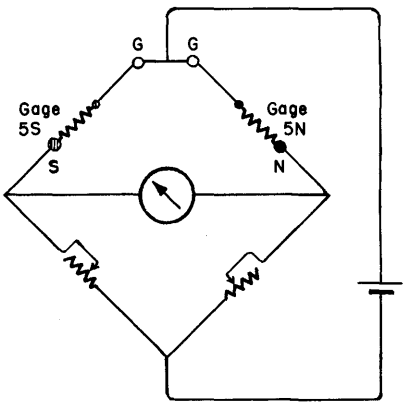

(b)
WHEATSTONE'S BRIDGE FORMED WHEN PLUG IS IN JACK NO. 5.

FIG. 7.(a),(b).
DIAGRAMS EXPLAINING SWITCH-BOARD CONNECTIONS.

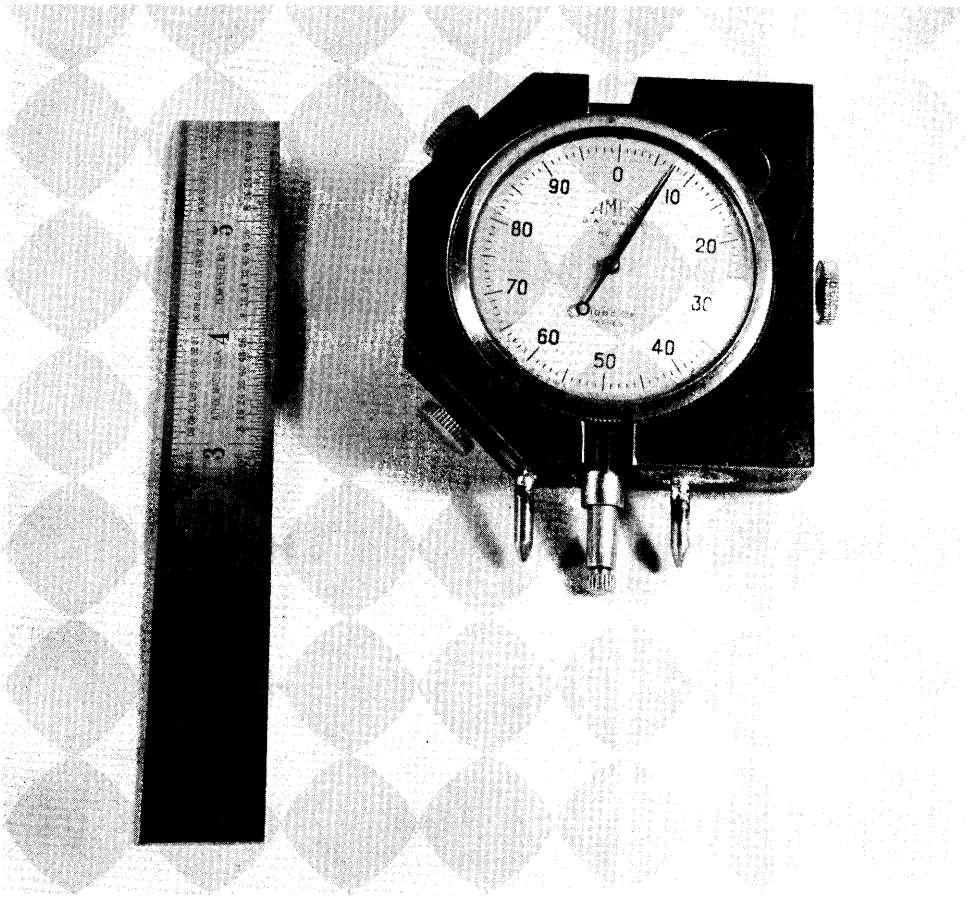

Figure 8. Instrument for curvature measurement.

Curvature readings--For measurements of curvatures of the deflected plate, a small instrument was built which made use of an Ames' dial reading to the nearest one-thousandth of an inch. A steel frame was designed to house the Ames' dial. This steel frame had on one side two small legs attached one inch apart; exactly midway between these two legs, there was an opening in the frame through which the movable leg of the Ames' dial could move when housed in the frame. Thus, when the Ames' dial was clamped within this frame by means of three screws, it became an instrument with three legs in a row: two fixed legs of same length one inch apart, and a movable leg exactly midway between the two fixed ones, the movement of which was shown by the Ames' dial. Figure 8 shows a view of the instrument. When the instrument was held with all its legs resting on a curved surface and with the central leg approximately perpendicular to the surface, the Ames' dial registered the movement of the center leg relative to the

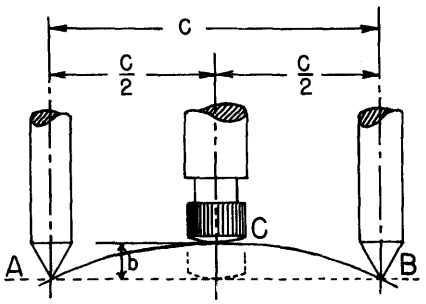

FIG. 9.

NOTATION FOR CURVATURE MEASUREMENT.

fixed outer legs. This movement would be approximately proportional to the curvature of the surface in the direction along which the three legs were aligned. The exact relation between this movement and curvature is found as follows.

If, in Figure 9, A and B are the positions of the fixed legs and C is that of the central movable leg, it follows that

$$\frac{1}{R} = \frac{d^2y}{dx^2} = \frac{8b}{c^2 + 4b^2}$$

where R is the radius of curvature. Since the distance c is equal to one inch and b^2 is extremely small, it follows that

$$\frac{1}{R} = 8b$$

If the radius of curvature is to be listed in feet and b is recorded as dial readings, it is seen that

$$\frac{1}{R} = 0.096b \qquad (16)$$

For measurements of curvature, the dial was set to zero when the legs were supported on a plain glass surface.

Test procedure--It was essential, for the study of variation of pressure due to wall movement, that immediately after the sand had been placed the wall should be approximately vertical along the portion in contact with the sand, allowing it to deflect subsequently by varying the restraining moment at the top. To achieve this object, a set of wooden bracings at different heights was provided on the side of the plate opposite to the sand filling, which kept the plate from deflecting while the sand was being filled. After the sand had been placed to a depth of 30 inches, just enough moment was applied to the top (by pulling the wire rope) to loosen the braces. The bracing was subsequently removed and the wall remained nearly vertical, due to the bending moment at the top. The wall was next allowed to deflect to different degrees by diminishing the bending moment at the top, by means of the hand wheel at the end of the wire rope. Since the turning of the hand wheel moved

the end of the wire rope very slowly, the change in tension was always slow and gradual, thus eliminating any vibration due to a sudden change in the bending moment at the top. Figure 10 shows the attachment of the wire rope at the top.

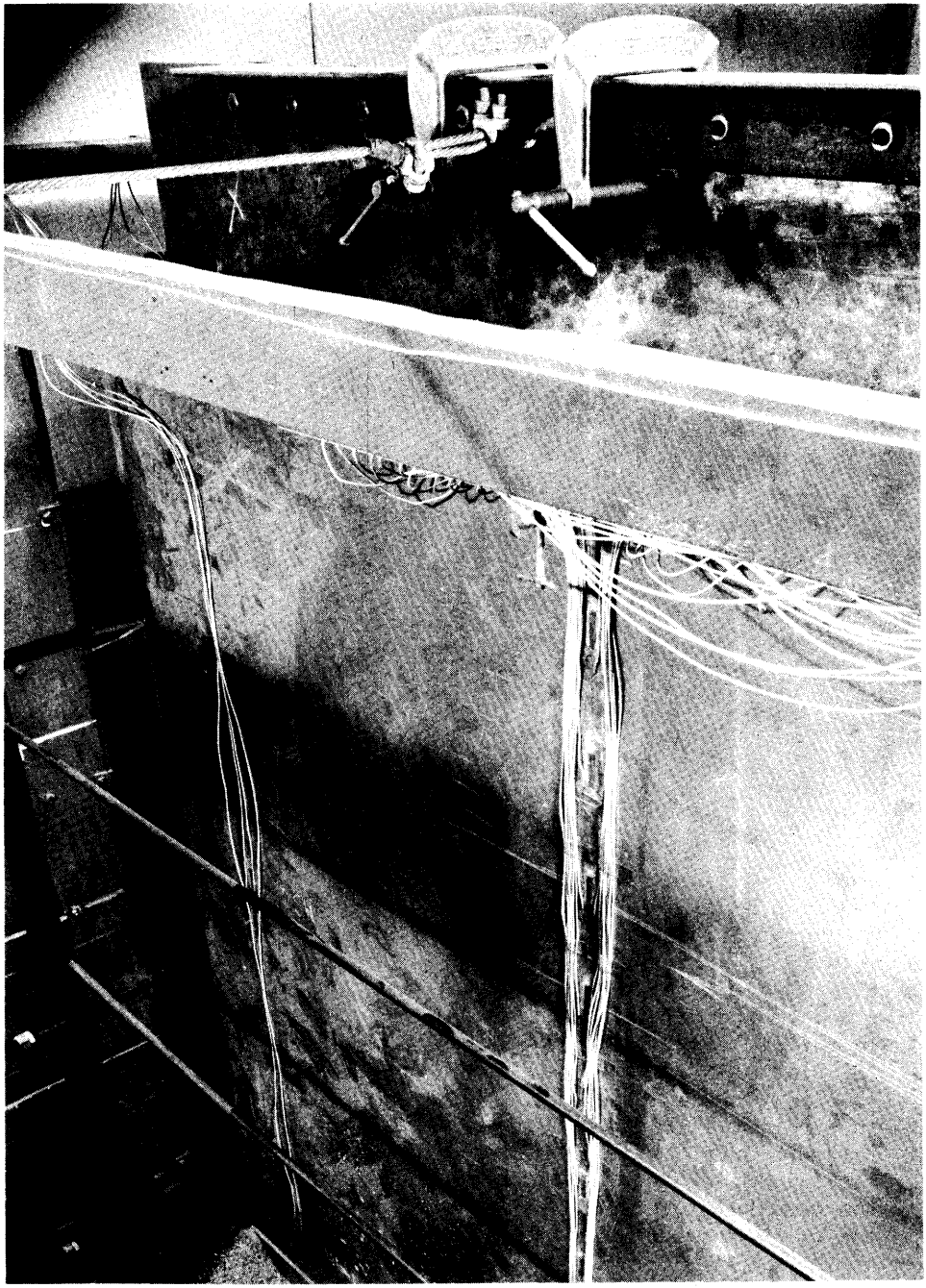

Figure 10. Top view of loaded membrane.

TEST OBSERVATIONS

Sequence of loading--Figure 11 shows the various loading conditions to which the aluminum plate in the earth pressure box was subjected. After the initial readings had been recorded for deflections, curvatures and strain gages, sand was filled behind the plate up to a height of 30 inches above the bottom. At the same, time a bending moment was applied at the top of such magnitude that the temporary bracings, which had been in place during the process of filling, could be readily removed. This is called Case 1.

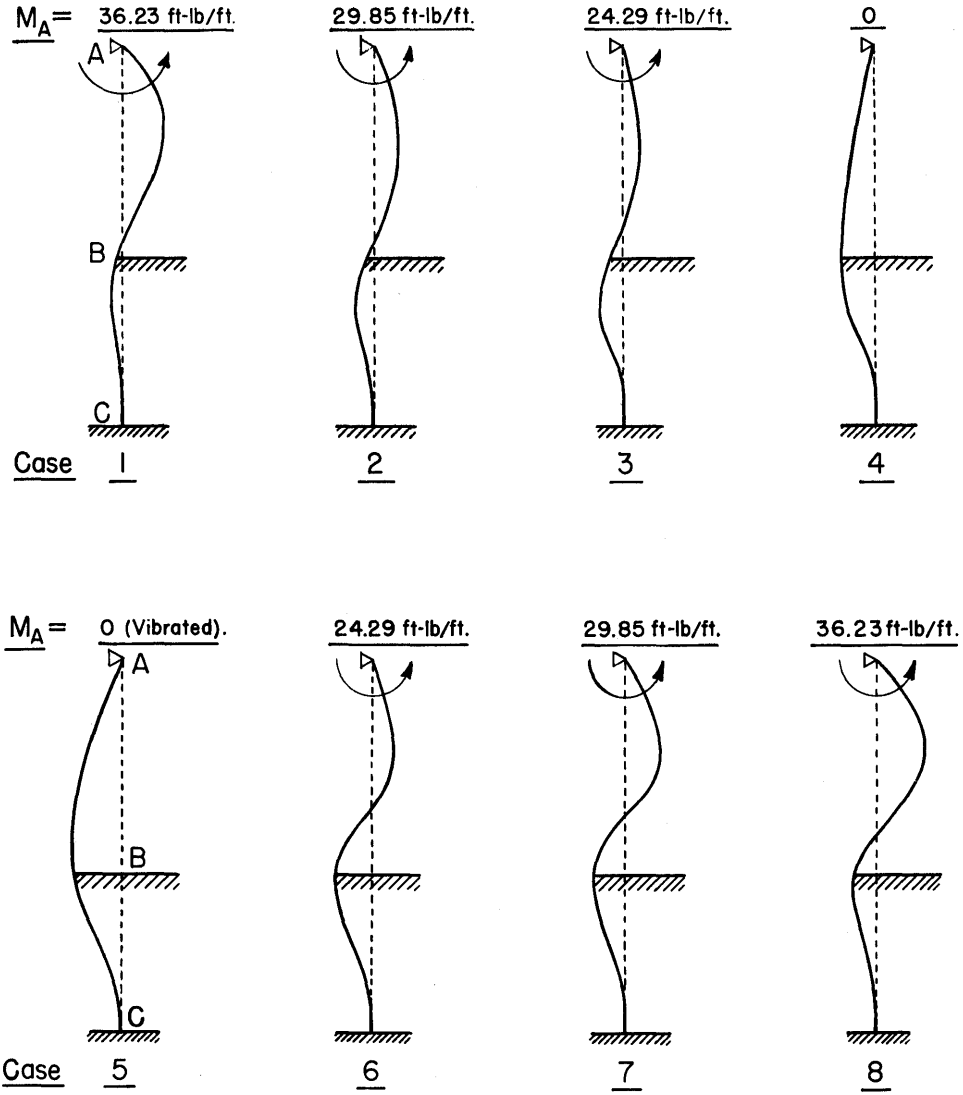

FIG. 11.

THE DIFFERENT CASES OF LOADING OBSERVED.

After completion of readings for Case 1, the restraining moment at the top was reduced by approximately twenty per cent. This further increased the deflections, and curvatures and strains also changed. This is called Case 2.

Subsequently, an additional reduction of the restraining moment, accompanied by increased deflections, was effected and is called Case 3.

The complete removal of any restraining moment at the top resulted in further change in strains and stresses and is called Case 4.

Next, the sand behind the plate was subjected to vibrations by delivering to both the plate and the sides of the box a rapid succession of blows from a hammer. This temporary reduction of internal friction in the sand increased the pressure and is labeled Case 5.

Finally, attempts were made to produce passive resistance in the sand by restoring in succession the restraining moments of Case 3, Case 2, and Case 1, so as to press the wall more and more against the mass of the sand. These three conditions have been named Case 6, Case 7, and Case 8, respectively.

Records of observations--The glass panes in the earth pressure box (see Figure 4) were provided with horizontal lines spaced vertically one inch. Deflections of the aluminum plate were measured along each one of these lines. Table II lists the averages of the deflections on both sides of the box at intervals of three inches. Positive quantities in this table indicate displacements in the same direction as the load is acting; negative quantities are in the opposite direction. Because the changes in the deflections due to the applications of moments in Cases 6, 7, and 8 were extremely small, only those of Cases 1 to 5 inclusive were recorded.

Curvature measurements were made at intervals of one inch along a vertical line on the unloaded side of the aluminum plate, three inches from the center line (which was occupied by the electrical strain gages). The measurements have been listed for intervals of three inches in Table III. Curvature measurements were recorded only for Cases 1 to 5 inclusive.

Net strain gage readings are listed in Table IV. The distances to the various gages are given in Figure 6. By recording for both initial and "under load" readings the differences between the outside and the inside strain gages, a magnification

TABLE II

Mean Net Deflection in Inches

Distance from top support (in.)	Case 1	2	3	4	5
3	-0.645	-0.625	-0.435	0.295	0.360
6	-1.100	-1.035	-0.740	0.590	0.720
9	-1.380	-1.320	-0.920	0.840	1.045
12	-1.545	-1.475	-1.015	1.075	1.340
15	-1.585	-1.520	-1.035	1.285	1.605
18	-1.535	-1.470	-0.980	1.470	1.830
21	-1.400	-1.340	-0.880	1.620	2.025
24	-1.200	-1.160	-0.740	1.740	2.175
27	-0.960	-0.920	-0.570	1.825	2.285
30	-0.700	-0.675	-0.385	1.875	2.350
33	-0.430	-0.415	-0.195	1.890	2.370
36	-0.170	-0.160	0	1.880	2.350
39	0.060	0.075	0.170	1.830	2.285
42	0.250	0.250	0.310	1.735	2.165
45	0.370	0.380	0.410	1.590	1.980
48	0.435	0.450	0.465	1.400	1.740
51	0.450	0.450	0.470	1.160	1.435
54	0.390	0.400	0.410	0.880	1.090
57	0.290	0.300	0.310	0.590	0.740
60	0.170	0.170	0.180	0.325	0.400
63	0.055	0.055	0.060	0.095	0.120
66	0	0	0	0	0

TABLE III

Curvature Readings
Rise, b, (see Figure 9) in 1/1000 Inch

Distance from top support (in.)	Case				
	1	2	3	4	5
3	+2.8	+2.5	+1.8	-0.2	-0.3
6	+2.6	+2.3	+1.7	-0.3	-0.3
9	+2.2	+1.9	+1.3	-0.5	-0.4
12	+1.7	+1.6	+1.1	-0.6	-0.6
15	+1.5	+1.4	+1.1	-0.4	-0.5
18	+0.9	+1.1	+0.8	-0.7	-0.7
21	+0.6	+0.8	+0.5	-0.8	-0.8
24	+0.3	+0.3	+0.2	-0.8	-0.9
27	+0.2	+0.1	0	-0.8	-0.9
30	+0.1	+0.1	-0.1	-0.7	-0.8
33	-0.4	-0.1	-0.1	-0.7	-0.8
36	-0.9	-0.8	-0.7	-0.9	-1.0
39	-1.2	-0.9	-0.8	-1.0	-1.0
42	-1.2	-1.1	-1.0	-0.9	-1.1
45	-1.2	-1.1	-0.9	-0.9	-0.9
48	-0.9	-0.8	-0.9	-0.7	-0.8
51	-0.8	-0.9	-0.8	-0.6	-0.6
54	-0.7	-0.9	-0.7	-0.3	-0.4
57	-0.5	-0.6	-0.6	-0.1	0
60	0	0	0	+0.7	+0.9
63	+0.5	+0.5	+0.6	+1.4	+1.7
66	--	--	--	--	--

TABLE IV

Net Strain Gage Readings in Micro-Inches Per Inch

Gage No.	Case 1	2	3	4	5	6	7	8
1	2443	2163	1493	- 237	- 273	1111	1566	2035
2	1990	1861	1330	- 338	- 402	740	1096	1430
3	1288	1272	951	- 430	- 540	142	402	613
4	1033	657	493	- 535	- 668	- 411	- 263	- 150
5	8	- 50	- 45	- 665	- 822	- 898	- 905	- 875
6	- 737	- 687	- 511	- 723	- 907	-1310	-1430	-1518
7	-1053	-1032	- 819	- 751	- 969	-1499	-1670	-1838
8	- 944	- 974	- 916	- 698	- 824	- 957	-1051	-1164
9	- 573	- 593	- 606	- 253	- 185	- 179	- 201	- 245
10	235	245	252	899	1132	1135	1150	1162
11	2006	1967	2032	3026	3166	3133	3139	3172
5E	- 7	18	24	- 596	- 757	- 768	- 752	- 731
5W	- 38	- 27	- 28	- 622	- 792	- 826	- 815	- 792
10E	185	199	179	911	1132	1162	1178	1182
10W	197	204	192	929	1186	1232	1248	1262

factor of two was obtained. For this reason, the quantities in Table IV will represent twice the actual strains.

Auxiliary tests--The modulus of elasticity for the aluminum was determined from a load-strain diagram of a small beam specimen having a width of 1 inch, a thickness of 1/8 inch, a span of 6 inches and loaded at the one-third points by a total load P. It is readily seen that

$$E = \frac{f}{\epsilon}$$

where ϵ is the maximum strain and f is the maximum bending stress.

Since

$$f = \frac{Mc}{I} = \frac{\frac{1}{2}P \times 2 \times \frac{1}{16}}{\frac{1}{12} \times (\frac{1}{8})^3} = 384\,P$$

the modulus of elasticity will be

$$E = 384 \frac{P}{\epsilon} \qquad (17)$$

The strains, ϵ, were recorded by electrical resistance gages and the relationship between P and ϵ was plotted as shown in Figure 12. The modulus of elasticity for the aluminum plate was found to equal 9,774,500 pounds per square inch.

In order to determine the angle of internal friction for the sand, direct shear tests were made in accordance with standard practice for these tests. These tests indicated a mean value ϕ = 35 degrees for this quantity.

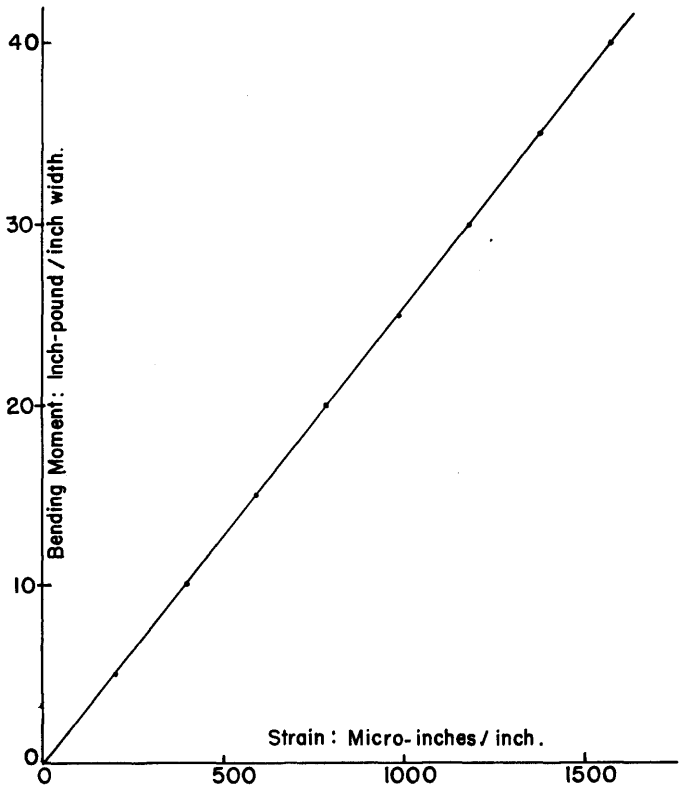

FIG. 12.

TEST RESULTS FOR DETERMINING THE MODULUS OF ELASTICITY.

COMPUTATIONS

The methods by which the load intensities can be determined from the observed deflections and strains have been explained in a previous section. The numerical calculations by which the load intensities were derived are listed in the following.

Use of deflections--Although the deflections of the aluminum plate were measured at intervals of one inch, it was decided to use only every third value for determination of the load diagram, and also to restrict the investigation to possible first and second degree polynomials. Thus, the expressions for the deflection become

$$y = A_1 f_1(x) + A_2 f_2(x) + M_A f_m(x) \qquad (18a)$$

between $x = 0$ and $x = 3$ feet, and

$$y_1 = A_1 F_1(x) + A_2 F_2(x) + M_A F_m(x) \qquad (18b)$$

between $x = 3$ feet and $x = 5.5$ feet.

The functions $f_1(x)$, $f_2(x)$,....$F_1(x)$, $F_2(x)$,....have already been evaluated [see Equations (11) and (12)]. In Table V numerical values have been found for these functions by substituting for x the distances 3 inches, 6 inches, 9 inches, 12 inches, 15 inches,.... Table V also lists the squares and cross-products of these numerical values.

The application of Equation (8) to Equations (18a) and (18b) gives

$$A_1\left[\sum\{f_1(x)\}^2 + \sum\{F_1(x)\}^2\right] + A_2\left[\sum f_1(x)\, f_2(x) + \sum F_1(x)\, F_2(x)\right]$$
$$= -M_A\left[\sum f_1(x)\, f_m(x) + \sum F_1(x)\, F_m(x)\right] + \sum y_{i,o} f_1(x) + \sum y_{i,o} F_1(x)$$

and (19)

$$A_1\left[\sum f_1(x)\, f_2(x) + \sum F_1(x)\, F_2(x)\right] + A_2\left[\sum\{f_2(x)\}^2 + \sum\{F_2(x)\}^2\right]$$
$$= -M_A\left[\sum f_2(x)\, f_m(x) + \sum F_2(x)\, F_m(x)\right] + \sum y_{i,o} f_2(x) + \sum y_{i,o} F_2(x)$$

TABLE V

Evaluation of Coefficients in Equation (19)

x	$f_1(x)$	$f_2(x)$	$[f_1(x)]^2$	$[f_2(x)]^2$	$f_1(x)f_2(x)$	$f_m(x)$	$f_1(x)f_m(x)$	$f_2(x)f_m(x)$
3	.160284	1.131420	.025691	1.280111	.181349	- .340176	- .054525	- .384882
6	.318096	2.246676	.101185	5.047553	.714659	- .617100	- .196297	- 1.386424
9	.470916	3.326340	.221762	11.064538	1.566427	- .835392	- .393399	- 2.778798
12	.616248	4.352352	.379762	18.942968	2.682128	- .999672	- .616046	- 4.350924
15	.751620	5.310876	.564933	28.205404	3.991761	-1.114572	- .837735	- 5.919354
18	.874536	6.180816	.764813	38.202486	5.405346	-1.184736	- 1.036094	- 7.322635
21	.982500	6.945900	.965306	48.245527	6.824347	-1.214760	- 1.193502	- 8.437601
24	1.073016	7.588656	1.151363	57.587700	8.142749	-1.209192	- 1.297482	- 9.176142
27	1.143600	8.091612	1.307821	65.474185	9.253567	-1.172988	- 1.341429	- 9.491364
30	1.191756	8.437272	1.420281	71.187559	10.055170	-1.110432	- 1.323364	- 9.369017
33	1.215000	8.608188	1.476225	74.100901	10.458948	-1.026264	- 1.246911	- 8.831427
36	1.210824	8.586864	1.466095	73.734233	10.397181	- .925128	- 1.120167	- 7.943948
	$F_1(x)$	$F_2(x)$	$[F_1(x)]^2$	$[F_2(x)]^2$	$F_1(x)F_2(x)$	$F_m(x)$	$F_1(x)F_m(x)$	$F_2(x)F_m(x)$
39	1.172664	8.354604	1.375141	69.799408	9.797143	- .811632	- .951772	- 6.780864
42	1.104972	7.899480	1.220963	62.401784	8.728704	- .690420	- .762895	- 5.453959
45	1.003572	7.210920	1.007157	51.997367	7.236677	- .566100	- .568122	- 4.082102
48	.869352	6.294204	.755773	39.617004	5.471879	- .443328	- .385408	- 2.790397
51	.706380	5.176272	.498973	26.793792	3.656415	- .326712	- .230783	- 1.691150
54	.522924	3.914052	.273450	15.319803	2.046752	- .220884	- .115506	- .864551
57	.332580	2.603136	.110609	6.776317	.865751	- .130476	- .043394	- .339647
60	.155316	1.387188	.024123	1.924291	.215450	- .060120	- .009338	- .083398
63	.018456	.467628	.000341	.218676	.008631	- .014436	- .000266	- .006751
SUM			15.111767	767.921798	107.701036		-13.724435	-97.488181

and computations in Table V reduce these equations to

$$15.1118\,A_1 + 107.7010\,A_2 = C_1$$
$$107.7010\,A_1 + 767.9218\,A_2 = C_2 \qquad (20)$$

where

$$C_1 = 13.7244\,M_A + \sum y_{i,o} f_1(x) + \sum y_{i,o} F_1(x)$$
$$C_2 = 97.4882\,M_A + \sum y_{i,o} f_2(x) + \sum y_{i,o} F_2(x) \qquad (21)$$

In the case of a first degree load curve, as represented by the first two terms of Equation (9), it is seen that

$$A_1 = 0.06617\,C_1$$
$$A_0 = -0.19851\,C_1 \qquad (22)$$

In the case of a second degree load curve both equations of Equation (19) are needed and, if solved, give

$$A_1 = 149.3393\,C_1 - 20.9448\,C_2$$
$$A_2 = -20.9448\,C_1 + 2.9388\,C_2 \qquad (23)$$
$$A_0 = 259.5147\,C_1 - 36.3852\,C_2$$

The values for C_1 and C_2 are computed by means of Table VI and Table VII for Cases 1 to 5 inclusive. The final equations for the first degree load curves may be found by the preceding expressions and will be

Case 1 $\quad p = 2.201\,(x - 3)$

Case 2 $\quad p = 1.749\,(x - 3)$

Case 3 $\quad p = 1.576\,(x - 3)$

TABLE VI

Evaluation of C_1 from Deflections in Table II

	$f_1(x)y_{i,o}$ or $F_1(x)y_{i,o}$				
	Case				
x	1	2	3	4	5
3	- .10338	- .10018	- .06972	.04728	.05770
6	- .34991	- .32923	- .23539	.18768	.22903
9	- .64986	- .62161	- .43324	.39557	.49211
12	- .95210	- .90897	- .62549	.66247	.82577
15	-1.19132	-1.14246	- .77793	.96583	1.20635
18	-1.34241	-1.28557	- .85705	1.28557	1.60040
21	-1.37550	-1.31655	- .86460	1.59165	1.98956
24	-1.28762	-1.24470	- .79403	1.86705	2.33381
27	-1.09786	-1.05211	- .65185	2.08707	2.61313
30	- .83423	- .80444	- .45883	2.23454	2.80063
33	- .52245	- .50423	- .23693	2.29635	2.87955
36	- .20584	- .19373	0	2.27635	2.84544
39	.07036	.08795	.19935	2.14598	2.67954
42	.27624	.27624	.34254	1.91713	2.39226
45	.37132	.38136	.41147	1.59568	1.98707
48	.37817	.39121	.40425	1.21709	1.51267
51	.31787	.31787	.33200	.81940	1.01366
54	.20394	.20917	.21440	.46017	.56999
57	.09645	.09977	.10310	.19622	.24611
60	.02640	.02640	.02796	.05048	.06213
63	.00102	.00102	.00111	.00175	.00222
SUM	-8.17071	-7.71277	-3.96889	24.30131	30.33911
$13.7244M_A$	41.43633	34.13952	27.78054	0	0
C_1	33.26562	26.42675	23.81165	24.30131	30.33911

TABLE VII

Evaluation of C_2 from Deflections in Table II

	$f_2(x)y_{i,o}$ or $F_2(x)y_{i,o}$				
	Case				
x	1	2	3	4	5
3	- .72977	- .70714	- .49217	.33377	.40731
6	- 2.47134	- 2.32531	- 1.66254	1.32554	1.61761
9	- 4.59035	- 4.39077	- 3.06023	2.79413	3.47603
12	- 6.72438	- 6.41972	- 4.41764	4.67878	5.83215
15	- 8.41774	- 8.07253	- 5.49676	6.82448	8.52396
18	- 9.48755	- 9.08580	- 6.05720	9.08580	11.31089
21	- 9.72426	- 9.30751	- 6.11239	11.25236	14.06545
24	- 9.10639	- 8.80284	- 5.61561	13.20426	16.50533
27	- 7.76795	- 7.44428	- 4.61222	14.76719	18.48933
30	- 5.90609	- 5.69516	- 3.24835	15.81989	19.82759
33	- 3.70152	- 3.57240	- 1.67860	16.26948	20.40141
36	- 1.46339	- 1.37731	0	16.18339	20.22924
39	.50128	.62660	1.42028	15.28893	19.09027
42	1.97487	1.97487	2.44884	13.70560	17.10237
45	2.66804	2.74015	2.95648	11.46536	14.27762
48	2.73798	2.83239	2.92681	8.81189	10.95192
51	2.32932	2.32932	2.43285	6.00448	7.42795
54	1.52648	1.56562	1.60476	3.44437	4.26632
57	.75491	.78094	.80697	1.53585	1.92632
60	.23582	.23582	.24969	.45084	.55488
63	.02572	.02572	.02806	.04443	.05612
SUM	-57.33631	-54.08933	-27.57896	172.75078	216.34004
$97.4882M_A$	294.33290	242.50175	197.33226	0	0
C_2	236.99659	188.41242	169.75330	172.75078	216.34004

Case 4 $p = 1.608\,(x - 3)$

Case 5 $p = 2.008\,(x - 3)$ (24)

Similarly the second degree curves, as found by Equation (23), will be

Case 1 $p = 4.010\,(x - 3) - 0.254\,(x^2 - 9)$

Case 2 $p = 0.284\,(x - 3) + 0.206\,(x^2 - 9)$

Case 3 $p = 0.560\,(x - 3) + 0.143\,(x^2 - 9)$

Case 4 $p = 10.903\,(x - 3) - 1.304\,(x^2 - 9)$ (25)

Case 5 $p = -0.385\,(x - 3) + 0.336\,(x^2 - 9)$

Curvature and moment--It was shown in a previous section [Equation (16)] that

$$\frac{d^2y}{dx^2} = 0.096\,b$$

where b indicates the curvature reading (see Figure 9) in one-thousandths of an inch. The above equation can also be written as

$$b = 10.417\,\frac{d^2y}{dx^2} \tag{26}$$

If Equations (13) and (14) are substituted for the second derivatives in Equation (26), it is found that for $0 < x < 3$ feet.

$$b = A_1 g_1(x) + A_2 g_2(x) + M_A g_m(x) \tag{27}$$

where

$$\begin{aligned} g_1(x) &= -0.13844\,x \\ g_2(x) &= -0.97088\,x \\ g_m(x) &= +0.94292 - 0.25713\,x \end{aligned} \tag{28}$$

and for 3 feet $< x <$ 5.5 feet

$$b = A_1 G_1(x) + A_2 G_2(x) + M_A G_m(x) \tag{29}$$

where

$$G_1(x) = -4.24269 + 4.10425x - 1.41450x^2 + .15708x^3$$

$$G_2(x) = -19.09294 + 15.99975x - 4.24350x^2 + .07875x^3$$

$$G_m(x) = g_m(x) \qquad (30)$$

In Table VIII, numerical values have been found for the functions in Equation (28) and Equation (30) by substituting for x the distances from the top A to the points where strain gages were located, and where curvature readings were obtained by interpolation in Table III. Table VIII also lists the squares and cross-products of these numerical values.

The application of Equation (8) to Equations (27) and (29) gives

$$A_1\left[\sum\{g_1(x)\}^2 + \sum\{G_1(x)\}^2\right] + A_2\left[\sum g_1(x)\,g_2(x) + \sum G_1(x)\,G_2(x)\right]$$

$$= -M_A\left[\sum g_1(x)\,g_m(x) + \sum G_1(x)\,G_m(x)\right] + \sum b_{i,o}g_1(x) + \sum b_{i,o}G_1(x)$$

and (31)

$$A_1\left[\sum g_1(x)\,g_2(x) + \sum G_1(x)\,G_2(x)\right] + A_2\left[\sum\{g_2(x)\}^2 + \sum\{G_2(x)\}^2\right]$$

$$= -M_A\left[\sum g_2(x)\,g_m(x) + \sum G_2(x)\,G_m(x)\right] + \sum b_{i,o}g_2(x) + \sum b_{i,o}G_2(x)$$

The computations in Table VIII reduce these equations to

$$4.037468A_1 + 29.813853A_2 = C'_1$$

$$29.813853A_1 + 220.342630A_2 = C'_2 \qquad (32)$$

TABLE VIII

Evaluation of Coefficients in Equation (27)

x	$g_1(x)$	$g_2(x)$	$[g_1(x)]^2$	$[g_2(x)]^2$	$g_1(x)g_2(x)$	$g_m(x)$	$g_1(x)g_m(x)$	$g_2(x)g_m(x)$
0.5417	- .074992	- .525923	.005624	.276595	.039440	.803632	- .060266	- .422649
1.0417	- .144210	- 1.011361	.020797	1.002850	.145849	.675070	- .097352	- .682739
1.5417	- .213429	- 1.496798	.045552	2.240404	.319460	.546507	- .116641	- .818011
2.0417	- .282648	- 1.982236	.079890	3.929258	.560275	.417945	- .118131	- .828465
2.5417	- .351867	- 2.467673	.123810	6.089410	.868292	.289382	- .101824	- .714100
	$G_1(x)$	$G_2(x)$	$[G_1(x)]^2$	$[G_2(x)]^2$	$G_1(x)G_2(x)$	$G_m(x)$	$G_1(x)G_m(x)$	$G_2(x)G_m(x)$
3.0417	- .425078	- 2.947615	.180691	8.688432	1.252966	.160820	- .068361	- .474034
3.5417	- .471089	- 3.266564	.221925	10.670440	1.538842	.032257	- .015196	- .105370
4.0417	- .389837	- 2.733985	.151973	7.474672	1.065808	- .096305	.037543	.263297
4.5417	- .063509	- .454088	.004033	.206196	.028839	- .224868	.014281	.102110
5.0417	.625707	4.587040	.391509	21.040938	2.870142	- .353430	- .221144	- 1.621199
5.5	1.676802	12.597755	2.811665	158.703436	21.123941	- .471271	- .790228	- 5.936954
SUM			4.037468	220.342630	29.813853		-1.537216	-11.238114

where

$$C_1' = 1.537216\,M_A + \sum b_{i,0}g_1(x) + \sum b_{i,0}G_1(x)$$

$$C_2' = 11.238114\,M_A + \sum b_{i,0}g_2(x) + \sum b_{i,0}G_2(x) \qquad (33)$$

In the case of a first degree load curve, as represented by the first two terms of Equation (9), it is seen that

$$A_1 = 0.247680\,C_1'$$

$$A_0 = -0.74304\,C_1' \qquad (34)$$

In the case of a second degree load curve, both equations of Equation (31) are needed and, if solved, give

$$A_0 = -516.383907\,C_1' + 69.829407\,C_2'$$

$$A_1 = 289.738880\,C_1' - 39.203637\,C_2'$$

$$A_2 = -39.203637\,C_1' + 5.309056\,C_2' \qquad (35)$$

The values for C_1' and C_2' are computed by means of Table IX and Table X for Cases 1 to 5 inclusive. The final expressions for the first degree load curves may be found by the preceding expressions and Equation (9), and will be

Case 1 $p = 1.913082\,(x - 3)$

Case 2 $p = 1.517864\,(x - 3)$

Case 3 $p = 1.575268\,(x - 3)$

Case 4 $p = 1.525746\,(x - 3)$ (36)

Case 5 $p = 1.944959\,(x - 3)$

Similarly, the second degree curves as found by Equation (35) will be

$$\text{Case 1} \quad p = 16.144574\,(x - 3) - 1.927297\,(x^2 - 9)$$

$$\text{Case 2} \quad p = 13.560225\,(x - 3) - 1.630832\,(x^2 - 9)$$

$$\text{Case 3} \quad p = 10.269795\,(x - 3) - 1.177461\,(x^2 - 9)$$

$$\text{Case 4} \quad p = 10.818757\,(x - 3) - 1.258508\,(x^2 - 9)$$

$$\text{Case 5} \quad p = 9.282910\,(x - 3) - 0.993757\,(x^2 - 9) \qquad (37)$$

TABLE IX

Evaluation of C_1' from Curvature Readings in Table III

	Case				
x	1	2	3	4	5
0.5417	- .187479	- .168731	- .119987	.022497	.022497
1.0417	- .237947	- .216315	- .144210	.093737	.100947
1.5417	- .181415	- .224101	- .160072	.149400	.149400
2.0417	- .084794	- .084794	- .056530	.211986	.240251
2.5417	0	- .017593	.035187	.246307	.281493
3.0417	.403824	.340062	.297555	.361316	.425078
3.5417	.565307	.518198	.471089	.413980	.494643
4.0417	.350853	.311869	.331361	.253394	.292378
4.5417	.044456	.053983	.047632	.019053	.022228
5.0417	.062571	.031285	.031285	.437995	.625707
5.5	2.347523	1.760642	2.515203	3.940485	5.198086
SUM	3.082899	2.304505	3.248513	6.160150	7.852708
$1.537216M_A$	4.641109	3.823823	3.111580	0	0
	7.724008	6.128328	6.360093	6.160150	7.852708

TABLE X

Evaluation of C_2' from Curvature readings in Table III

	Case				
x	1	2	3	4	5
0.5417	-1.314808	-1.183327	- .841477	.157777	.157777
1.0417	-1.668745	-1.517041	-1.011361	.657384	.707952
1.5417	-1.272278	-1.571638	-1.122599	1.047759	1.047759
2.0417	- .594671	- .594671	- .396447	1.486677	1.684900
2.5417	0	- .123384	.246767	1.727371	1.974138
3.0417	2.800234	2.358092	2.063330	2.505472	2.947615
3.5417	3.919877	3.593220	3.266564	2.939908	3.429892
4.0417	2.460586	2.187188	2.323887	1.777090	2.050488
4.5417	.317862	.385975	.340566	.136226	.158931
5.0417	.458704	.229352	.229352	3.210928	4.587040
5.5	17.636857	13.227643	18.896633	29.604725	39.053041
SUM	22.743618	16.991409	23.995215	45.251317	57.799533
$11.238113M_A$	33.929717	27.954795	22.747806	0	0
	56.673335	44.946204	46.743021	45.251317	57.799533

The numerical work for curvature can be applied directly to the transformation of strain gage readings into pressure intensities. A comparison of Equations (15) and (16) indicates that all numerical values pertaining to strains can be obtained by expressing the measured strains, e, in thousandths of an inch per inch. Thus, corresponding to Equation (33), will be the following:

$$C_1' = 1.537216\,M_A + \sum e_{i,o}\,g_1(x) + \sum e_{i,o}\,G_1(x)$$
$$C_2' = 11.23811\,M_A + \sum e_{i,o}\,g_2(x) + \sum e_{i,o}\,G_2(x) \qquad (38)$$

The values for C_1' and C_2', pertaining to strain gage readings, have been computed in Table XI and Table XII for Cases 1 to 8 inclusive. The final expressions for the first degree load curves will be

$$\begin{aligned}
&\text{Case 1} \quad p = 2.062365\,(x - 3)\\
&\text{Case 2} \quad p = 1.882746\,(x - 3)\\
&\text{Case 3} \quad p = 1.745018\,(x - 3)\\
&\text{Case 4} \quad p = 1.765985\,(x - 3)\\
&\text{Case 5} \quad p = 1.947720\,(x - 3)\\
&\text{Case 6} \quad p = 2.708234\,(x - 3)\\
&\text{Case 7} \quad p = 2.886856\,(x - 3)\\
&\text{Case 8} \quad p = 3.103020\,(x - 3)
\end{aligned} \tag{39}$$

The final equations for the second degree load curve will be

$$\begin{aligned}
&\text{Case 1} \quad p = 3.627848\,(x - 3) - 0.212036\,(x^2 - 9)\\
&\text{Case 2} \quad p = 3.535721\,(x - 3) - 0.223881\,(x^2 - 9)\\
&\text{Case 3} \quad p = 0.882288\,(x - 3) + 0.116804\,(x^2 - 9)\\
&\text{Case 4} \quad p = 1.032630\,(x - 3) + 0.099283\,(x^2 - 9)\\
&\text{Case 5} \quad p = 6.063074\,(x - 3) - 0.557344\,(x^2 - 9)\\
&\text{Case 6} \quad p = 17.573398\,(x - 3) - 2.013123\,(x^2 - 9)\\
&\text{Case 7} \quad p = 20.019255\,(x - 3) - 2.320161\,(x^2 - 9)\\
&\text{Case 8} \quad p = 22.541146\,(x - 3) - 2.632412\,(x^2 - 9)
\end{aligned} \tag{40}$$

TABLE XI

Evaluation of C_1' from Strain Gage Readings in Table IV

	Case							
x (ft)	1	2	3	4	5	6	7	8
0.5417	-.183204	-.162207	-.111962	.017773	.020473	-.083316	-.117437	-.152608
1.0417	-.286978	-.268375	-.191800	.048743	.057973	-.106716	-.158054	-.206221
1.5417	-.274897	-.271482	-.202971	.091775	.115251	-.030307	-.085798	-.130832
2.0417	-.291975	-.185700	-.139345	.151217	.188809	.116168	.074336	.042397
2.5417	-.002815	.017593	.015834	.233991	.289234	.315967	.318439	.307883
3.0417	.313283	.292029	.217215	.307331	.385546	.556852	.607862	.645269
3.5417	.496057	.486164	.385822	.353788	.456485	.706162	.786719	.865862
4.0417	.368006	.379701	.357090	.272106	.321225	.373074	.409718	.453770
4.5417	.036391	.037661	.038487	.016068	.011749	.011368	.012765	.015560
5.0417	.147041	.153298	.157678	.562510	.708300	.710177	.719563	.727071
5.5	3.364714	3.299022	3.407825	5.074787	5.308818	5.253389	5.263653	5.319082
SUM	3.685623	3.777704	3.933873	7.130107	7.863857	7.822727	7.831766	7.887233
$1.537216M_A$	4.641109	3.823823	3.111580	0	0	3.111580	3.823823	4.641109
TOTAL	8.326723	7.601527	7.045453	7.130107	7.863857	10.934407	11.655589	12.528342

TABLE XII

Evaluation of C_2' from Strain Gage Readings in Table IV

x (ft)	Case 1	2	3	4	5	6	7	8
0.5417	-1.284830	-1.137571	- .785203	.124644	.143577	- .584300	- .823595	-1.070253
1.0417	-2.012607	-1.882142	-1.345109	.341840	.406567	- .748407	-1.108451	-1.446246
1.5417	-1.927876	-1.903927	-1.423455	.643623	.808271	- .212545	- .601713	- .917537
2.0417	-2.047649	-1.302329	- .977242	1.060496	1.324133	.814699	.521328	.297335
2.5417	- .019741	.123384	.111045	1.641003	2.028427	2.215970	2.233244	2.159214
3.0417	2.172392	2.025011	1.506231	2.131125	2.673486	3.861375	4.215089	4.474479
3.5417	3.439692	3.371094	2.675316	2.453189	3.165300	4.896579	5.455162	6.003944
4.0417	2.580881	2.662901	2.504330	1.908321	2.252803	2.616423	2.873418	3.182358
4.5417	.260192	.269274	.275177	.114834	.084006	.081282	.091272	.111252
5.0417	1.077954	1.123825	1.155934	4.123749	5.192530	5.206291	5.275096	5.330141
5.5	25.278984	24.785435	25.602876	38.126692	39.884962	39.468530	39.545646	39.962079
SUM	27.517392	28.134955	29.299900	52.669516	57.964062	57.615897	57.676496	58.087425
$11.238113M_A$	33.929717	27.954795	22.747806	0	0	22.747806	27.954795	33.929717
TOTAL	61.447109	56.089750	52.047706	52.669516	57.964062	80.363703	85.631291	92.017142

COMPARISON OF RESULTS

In the foregoing it has been shown that the test results can be interpreted in terms of a polynomial of any desired degree. The higher the degree of the polynomial, the more coefficients will be needed. It follows that the higher the degree, the greater will also be the numerical work required for determination of the necessary coefficients.

The curves thus arrived at are each more representative of the observational data than any other curve of the same degree. In order to determine which degree polynomial is the best fitting, it becomes necessary to compute for all the different degrees the quantity

$$S = \sum (y_i - y_{i,o})^2 \qquad (41)$$

These quantities are compared and the degree polynomial, for which this sum of the squares of the differences between the theoretical and the observed values is a minimum, is listed for the first five cases, as found from measured deflections and strains, in Table XIII.

Deflections and strains—Considerable agreement was found to exist between the pressure diagrams derived by observed deflections and recorded bending strains. In Figure 13 and Figure 14 are plotted the diagrams for the first five cases as shown in Figure 11. For Case 1, it will be recalled that the deflections of the aluminum membrane were reduced by the application of a restraining moment at the top of the membrane. The two curves corresponding to this condition "bulge" away from the membrane and thus indicate an accumulation of pressure near the center portion of the loaded part.

As the restraining moment is decreased (Cases 2 and 3) and finally is removed (Case 4), there is a gradual reduction of pressure. The consolidation of the sand, which resulted from prolonged vibrations, caused an increase in the pressure (Case 5).

In both Figures 13 and 14 the conventional pressure, according to Rankine's theory, has been plotted as a dotted line. With a unit weight of 108 pounds per cubic foot and an angle of internal friction of 35 degrees (as found by direct measurements), the maximum pressure at the bottom of the box will be

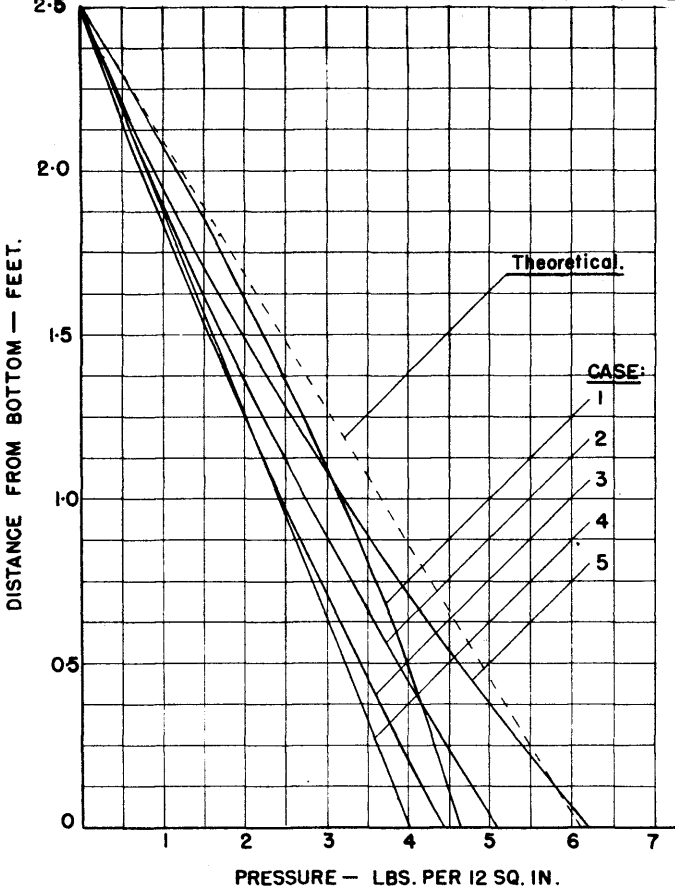

FIG. 13.

PRESSURE DIAGRAMS OBTAINED FROM MEASURED DEFLECTIONS.

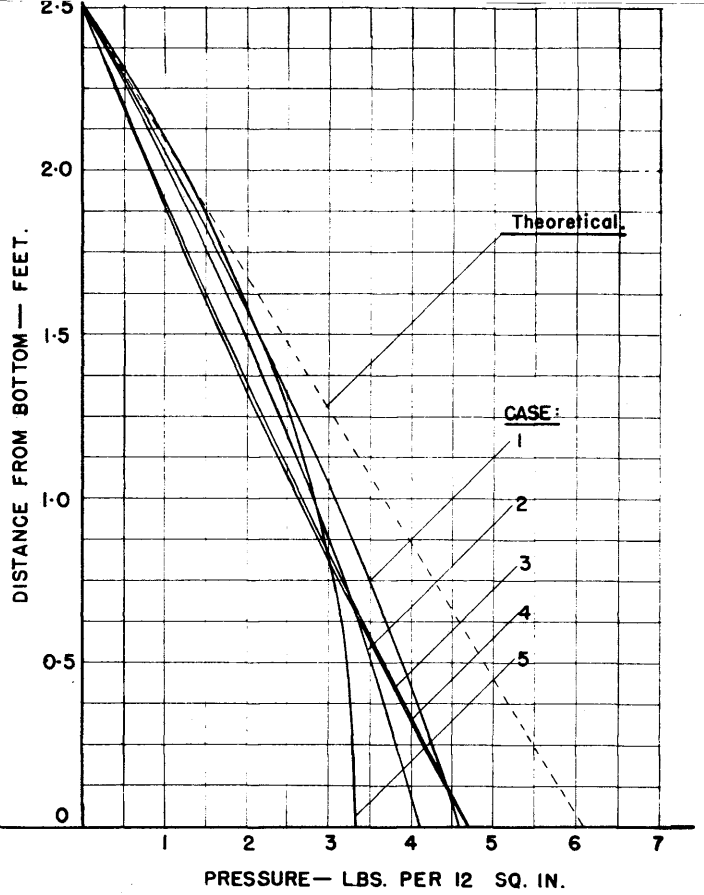

FIG. 14

PRESSURE DIAGRAMS OBTAINED FROM MEASURED STRAINS.

$$108 \times 2.5 \times \tan^2\left(45° - \frac{35°}{2}\right) = 73.2 \text{ lbs. per sq. ft.}$$

$$= 6.1 \text{ lbs. per lin. ft., per in. width of plate.}$$

Of the five curves in Figure 13 all but one came out parabolas, but it is interesting to note that they all have very slight curvatures and are very close to straight lines. Furthermore, Table XIIIA indicates that the differences in fitness between the straight lines and the parabolas are, except in Case 4, very small.

Every one of the five curves in Figure 14 is a parabola, but according to Table XIIIB the corresponding straight lines all, except for Case 5, fit for all practical purposes as well as the parabolas. The curvatures of the parabolas for the first four cases are extremely slight, making them appear almost like straight lines.

Passive pressures--A reapplication of the restraining moment at the top of the membrane (see Figure 11, Cases 6, 7, and 8) reduced the deflections by forcing it against the fill. The result was a very large increase in pressure, as shown in Figure 15. The increases were especially large where the deflections were reduced the most, near the center of the plate.

A comparison between straight lines and parabolas by least squares left no doubt as to the best fit; the sums of the squares for the former were from two to three times those for the latter.

Curvature--The results from the curvature measurements are not considered satisfactory. In order to make this report complete, they are presented in Figure 16. In all cases the parabola fitted better than the straight line, but due to insufficient accuracy of the instrument (Figure 8) which was used for measurements, these parabolas all have very sharp curvatures and two of them even show negative pressures at the bottom. It is believed, however, that an improved design of the curvature indicator, using a more accurate dial, will give results comparable to those obtained from measured deflections and bending strains.

TABLE XIII

A. By Measured Deflections

Quantities $\sum (y_i - y_{i,o})^2$.

CASE	1	2	3	4	5
1st. Degree	.198	.039	.023	.064	.091
2nd. Degree	.138	.024	.016	.788	.086

B. By Measured Strains

Quantities Proportional to $\sum \left[\left(\frac{d^2y}{dx^2}\right)_i - \left(\frac{d^2y}{dx^2}\right)_{i,o}\right]^2$.

CASE	1	2	3	4	5
1st. Degree	.476	.575	.148	.098	.113
2nd. Degree	.467	.565	.146	.096	.055

C. By Measured Curvatures

Quantities Proportional to $\sum \left[\left(\frac{d^2y}{dx^2}\right)_i - \left(\frac{d^2y}{dx^2}\right)_{i,o}\right]^2$.

CASE	1	2	3	4	5
1st. Degree	.974	.813	.406	.670	.532
2nd. Degree	.452	.407	.172	.416	.369

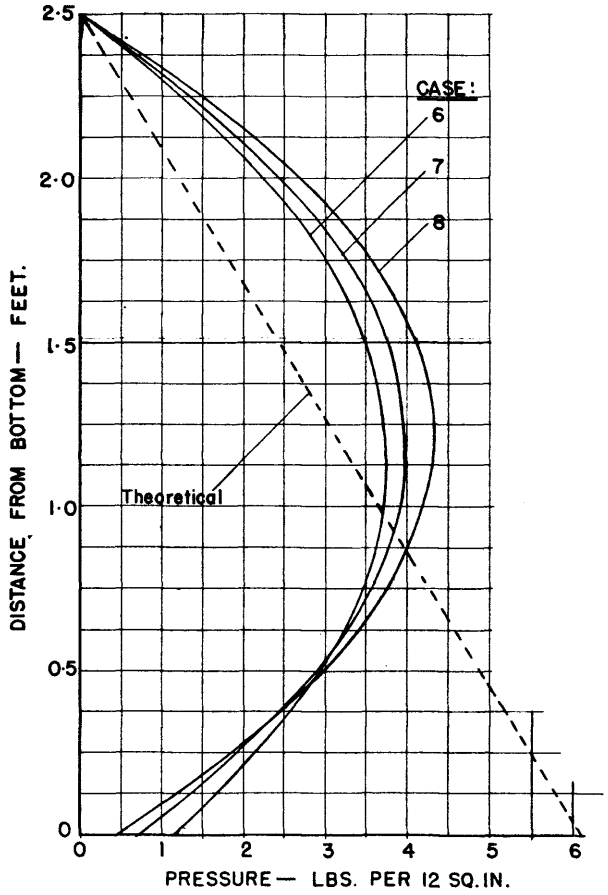

FIG. 15

PRESSURE DIAGRAMS OBTAINED FROM MEASURED STRAINS

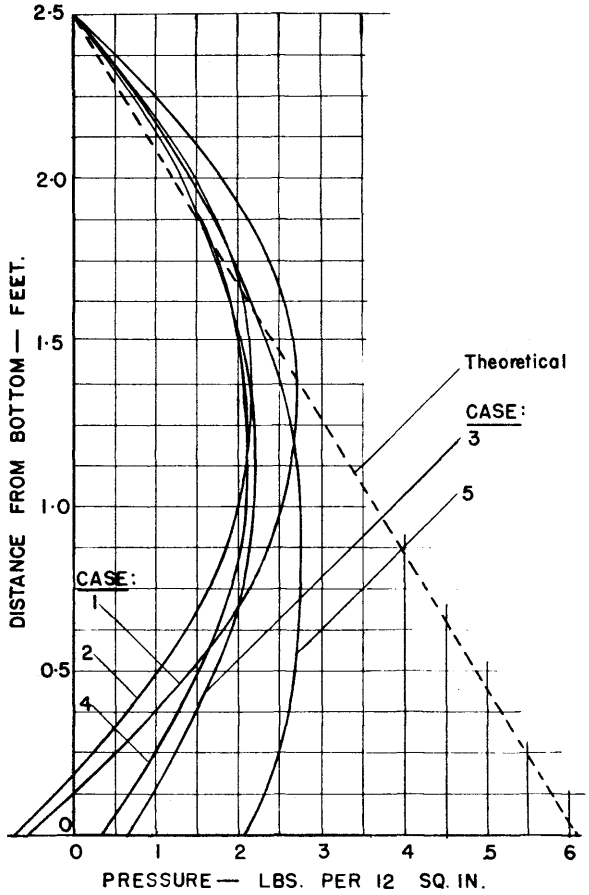

FIG. 16

PRESSURE DIAGRAMS OBTAINED FROM MEASURED CURVATURES

The Engineering Experiment Station of the University of Minnesota was established by an act of the Board of Regents on December 13, 1921.

The purpose of the Station is to advance research and graduate study in the Institute of Technology, to conduct scientific and industrial investigations, and to cooperate with governmental bodies, technical societies, associations, industries, or public utilities in the solution of technical problems. The results of scientific investigations will be published in the form of bulletins and technical papers. Information which is of general interest and yet not the result of original research may be distributed in the form of circulars.

For a complete list of publications or other information concerning the work of the Station, address the Director of the Engineering Experiment Station.

BULLETINS AVAILABLE

12. Thermal Conductivity of Building Materials, by Frank B. Rowley and A. B. Algren. x + 134 pages, 109 illustrations. 1937. $1.50. (Purchased through University Press.)
14. Square Sections of Reinforced Concrete under Thrust and Nonsymmetrical Bending, by Paul Andersen. vi + 42 pages, 8 figures, 23 diagrams. 1939.
15. Laboratory Studies of Asphalt Cements, by Fred C. Lang and T. W. Thomas. x + 96 pages, 43 illustrations. 1939.
16. Factors Affecting the Performance and Rating of Air Filters, by Frank B. Rowley and Richard C. Jordan. viii + 54 pages, 21 illustrations. 1939.
18. Condensation of Moisture and Its Relation to Building Construction and Operation, by Frank B. Rowley, A. B. Algren, and C. E. Lund. vi + 69 pages, 28 illustrations. 1941.
19. Pulp, Paper, and Insulation Mill Waste Analysis, by Frank B. Rowley, Richard C. Jordan, Reuben M. Olson, and Richard F. Huettl. vi + 55 pages, 34 illustrations. 1942.
20. Conservation of Fuel, by Frank B. Rowley, Richard C. Jordan, and C. E. Lund. vi + 61 pages, 22 illustrations, 17 tables. 1943.
21. Aids to Technical Writing, by R. C. Jordan and M. J. Edwards. viii + 112 pages, 60 illustrations, 13 tables. May, 1944.
24. Factors Affecting Heat Transmission through Insulated Walls, by Frank B. Rowley and C. E. Lund. iv + 25 pages, 8 illustrations, 8 tables. April, 1946.
25. Vapor Resistant Coatings for Structural Insulating Board, by Frank B. Rowley, M. H. LaJoy and E. T. Erickson. vi + 31 pages, 9 illustrations, 10 tables. September, 1946.

26. Moisture and Temperature Control in Buildings Utilizing Structural Insulating Board, by Frank B. Rowley, Millard H. LaJoy, and Einar T. Erickson. vi + 38 pages, 16 illustrations, 8 tables. July, 1947.
27. Water Permeability of Structural Clay Tile Facing Walls, by J. A. Wise. iv + 32 pages, 26 illustrations, 4 tables. August, 1948.
28. Thermal Properties of Soils, by Miles S. Kersten. xiv + 227 pages, 138 figures, 15 tables, 5 plates. June, 1949.
29. Proceedings of the Symposium on Engineering Research, edited by C. E. Lund. x + 110 pages. August, 1949.
30. Some Causes of Paint Peeling, by Frank B. Rowley and Millard H. LaJoy. vi + 34 pages, 23 illustrations, 11 tables. September, 1949.

TECHNICAL PAPERS AVAILABLE

1. Condensation within Walls, by Frank B. Rowley, A. B. Algren, and C. E. Lund. 12 pages. January, 1938.
3. Air Filter Performance as Affected by Kind of Dust, Rate of Dust Feed, and Air Velocity through Filter, by Frank B. Rowley and R. C. Jordan. 10 pages. June, 1938.
32. Construction and Operation of a 15-inch Cupola, by Fulton Holtby. 4 pages. August, 1941.
42. Abnormal Currents in Distribution Transformers Due to Lightning, by J. M. Bryant and M. Newman. 5 pages. September, 1942.
46. Discoloration Method of Rating Air Filter, by Frank B. Rowley and R. C. Jordan. 10 pages. September, 1943.
48. Valve Guide Leakage in an Automotive Engine, by M. A. Lindeman and B. J. Robertson. 22 pages. May, 1944.
52. Carbon Dioxide Variation in a Vented Stack, by M. H. LaJoy. 27 pages. May, 1945.
53. Thermal Conductivity of Insulating Material at Low Mean Temperatures, by Frank B. Rowley, R. C. Jordan, and R. M. Lander. 6 pages. December, 1945.
56. Calculation of Bearing Capacities of Footings by Circular Arcs, by Paul Andersen. 3 pages. June, 1946.
60. Comfort Reactions of 275 Workmen during Occupancy of Air-Conditioned Offices, by Frank B. Rowley, R. C. Jordan, and W. E. Snyder. 4 pages. June, 1947.
62. A Statistical Analysis of Water Works Data for 1945, by G. J. Schroepfer, A. S. Johnson, H. F. Seidel, and M. B. Al-Hakim. 32 pages. October, 1948.
63. Theory and Use of Capillary Tube Expansion Device, by M. M. Bolstad and R. C. Jordan. 6 pages. December, 1948.
64. Heating Panel Time Response Study, by A. B. Algren and Ben Ciscel. 4 pages. March, 1949.

65. Impact Strength Testing Machine, by Frank B. Rowley and M. H. LaJoy. 16 pages. June, 1949.
66. Ground Temperatures as Affected by Weather Conditions, by A. B. Algren. 6 pages. June, 1949.
67. Theory and Use of Capillary Tube Expansion Device, Part II, Non-adiabatic Flow, by M. M. Bolstad and R. C. Jordan. 7 pages. June, 1949.
68. Thermal Conductivity of Soils, by M. S. Kersten. July, 1949.
69. Specific Heat Tests on Soils, by M. S. Kersten. 5 pages. May, 1949.
72. Resistance Gradients through Viscous Coated Air Filters, by Frank B. Rowley and R. C. Jordan. 8 pages. December, 1949.

CIRCULARS AVAILABLE

3. A Five-Year Mechanical Engineering Curriculum, by R. C. Jordan. 5 pages. January, 1947.
4. The Transport of Solid Particles in a Fluid Stream--A Bibliography with Abstracts, by Wickliffe B. Hendry. 28 pages. October, 1949.